Expanded View Figures

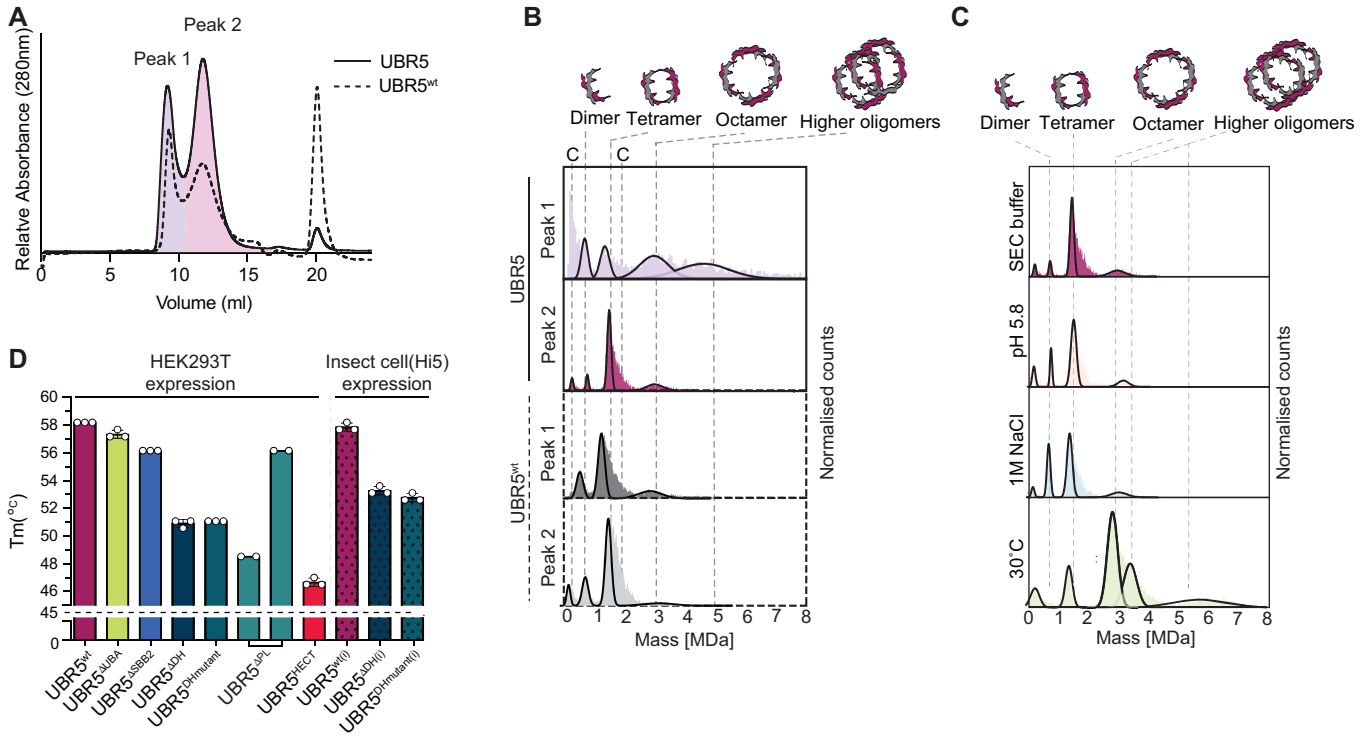

Figure EV1. Characterisation of UBR5 oligomers.

A SEC profiles of two full-length UBR5 constructs used in this study.

B Mass distributions and respective oligomeric states adopted by UBR5 constructs from SEC peaks shown in (A), measured using MP. Y-axes were normalised equally to a scale of 0–0.05 of normalised counts. Contaminant peaks and shoulders are annotated with "C".

C Mass distribution of UBR5 from the second SEC elution peak shown in (A), diluted in buffers of different conditions, measured with MP. Axes and annotations as in (B).

D Melting temperatures of all proteins expressed in this study, measured by ThermoFluor. Mean and standard deviation of three technical replicates are plotted. For $UBR5^{\Delta PL}$, four replicates were measured and plotted as two peaks.

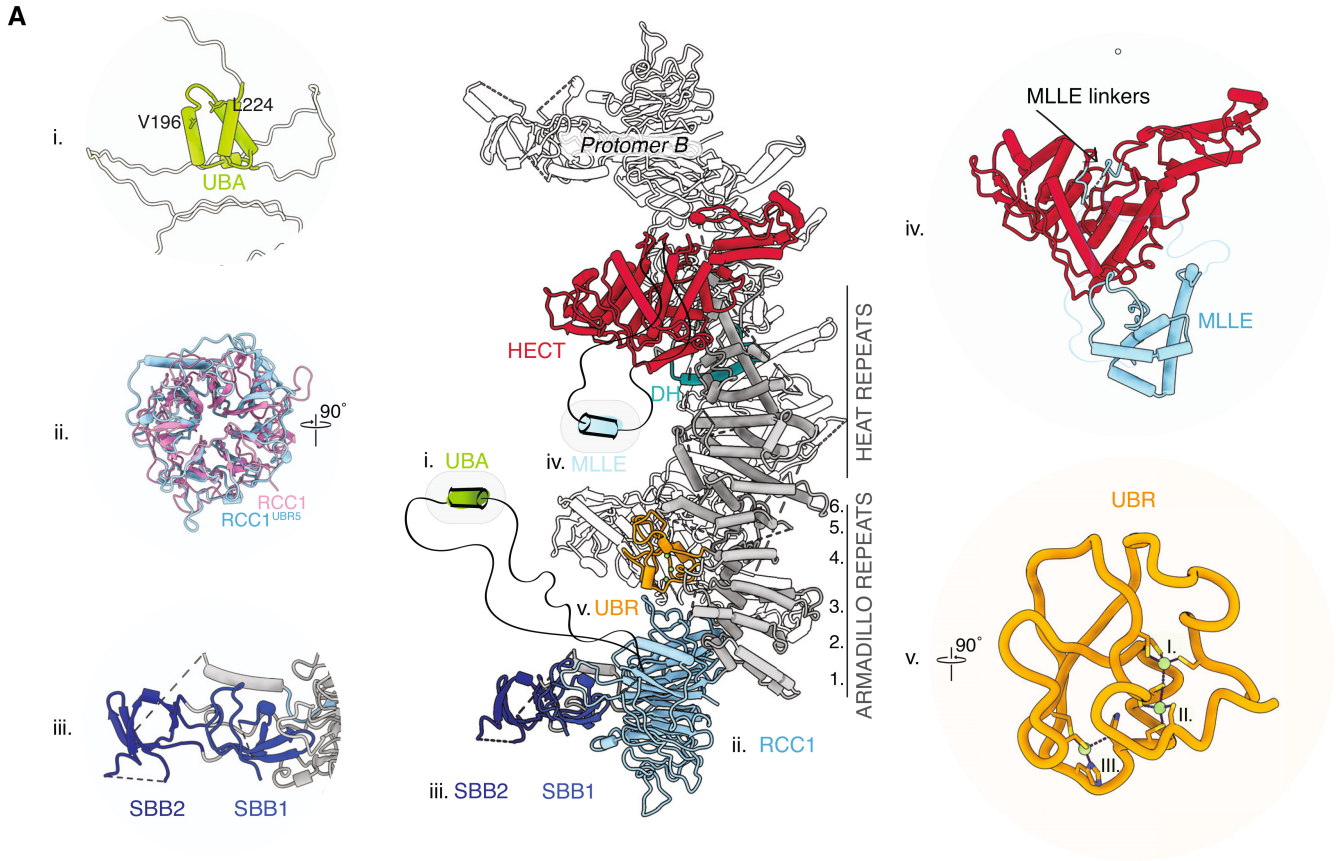
A
i.
V196
L224
UBA
ii.
90˚
RCC1
RCC1 UBR5
iii.
SBB2
SBB1
Protomer B
HECT
DH
i. UBA
iv. MLLE
v. UBR
ii. RCC1
iii. SBB2
SBB1
HEAT REPEATS
ARMADILLO REPEATS
6.
5.
4.
3.
2.
1.
iv.
MLLE linkers
MLLE
UBR
v.
90˚
I.
II.
III.

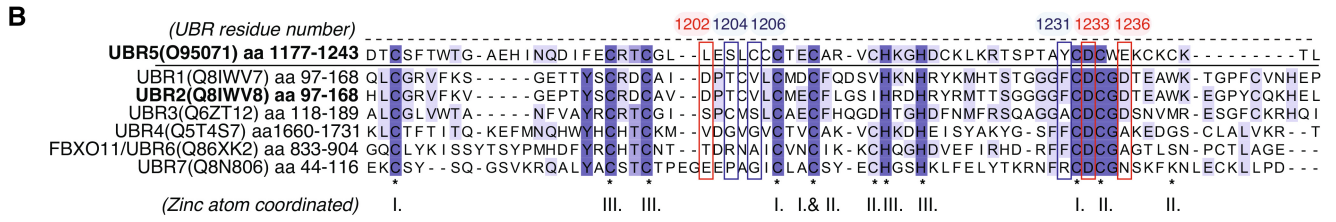
B
(UBR residue number)
1202 1204 1206
1231 1233 1236
UBR5(O95071) aa 1177-1243 DTCSFTWTG-AEHINQDIFECRTCGL--LESLCCCTECAR-VCHKGHDCKLKRTSPTAYCDCWEKCKCK---------TL
UBR1(Q8IWV7) aa 97-168 QLCGRVFKS-----GETTYSCRDCAI--DPTCVLCMDCFQDSVHKNHRYKMHTSTGGGFCDCGDTEAWK-TGPFCVNHEP
UBR2(Q8IWV8) aa 97-168 HLCGRVFKV-----GEPTYSCRDCAV--DPTCVLCMECFLGSIHRDHRYRMTTSGGGGFCDCGDTEAWK-EGPYCQKHEL
UBR3(Q6ZT12) aa 118-189 ALCGLVWTA-----NFVAYRCRTCGI--SPCMSLCAECFHQGDHTGHDFNMFRSQAGGACDCGDSNVMR-ESGFCKRHQI
UBR4(Q5T4S7) aa1660-1731 KLCTFTITQ-KEFMNQHWYHCHTCKM--VDGVGVCTVCAK-VCHKDHEISYAKYG-SFFCDCGAKEDGS-CLALVKR--T
FBXO11/UBR6(Q86XK2) aa 833-904 GQCLYKISSYTSYPMHDFYRCHTCNT--TDRNAICVNCIK-KCHQGHDVEFIRHD-RFFCDCGAGTLSN-PCTLAGE---
UBR7(Q8N806) aa 44-116 EKCSY--SQ-GSVKRQALYACSTCTPEGEEPAGICLACSY-ECHGSHKLFELYTKRNFRCDCGNSKFKNLECKLLPD---
(Zinc atom coordinated) I. III. III. I. I.& II. II.III. III. I. II. II.

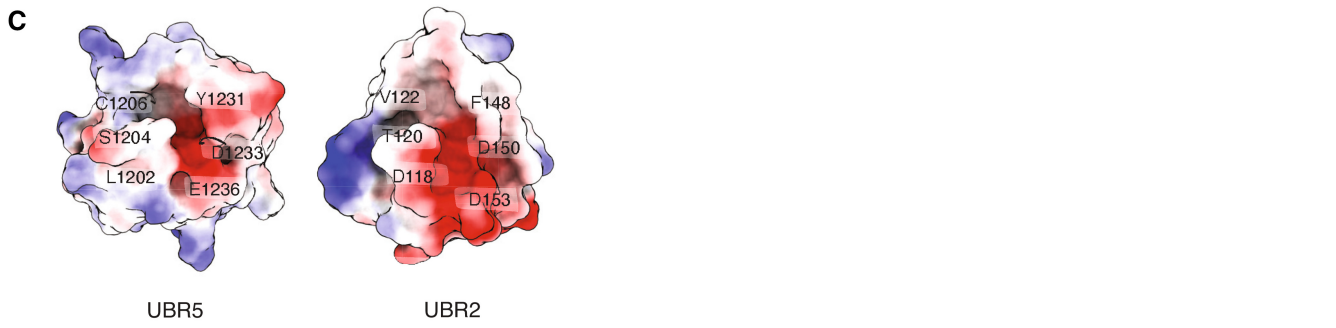
C
C1206
Y1231
S1204
D1233
L1202
E1236
V122
F148
T120
D150
D118
D153
UBR5
UBR2

Figure EV2.

Figure EV2. Insights into UBR5 structural features.

A All known putative substrate-recognition motifs of UBR5, colour coded as in Fig 2A, and their enhanced views (i–v). UBA and MLLE, two domains with no density in our reconstructions, are illustrated as schematics. Their enhanced views are based on the AlphaFold2-predicted UBR5 model. Panel i shows the UBA domain with surrounding linkers, two residues highlighted were found crucial for ubiquitin binding. Panel ii shows an overlay of UBR5 RCC1 domain with the RCC1 crystal structure (PDB:1A12). Panel iii shows two tandem SBB domains of UBR5. Panel iv represents an enhanced view of the MLLE linkers resolved in our cryo-EM density, with the MLLE domain itself placed based on AlphaFold2 predictions. Panel v represents an enhanced view of the UBR domain, showing three zinc atoms which stabilise the domain's tertiary fold. Rotation arrows represent positions of the domains with respect to the central full-length model.

B Sequence comparison of UBR boxes across seven human UBR E3 ligases. Residues mediating the contacts with the N-degron are highlighted in boxes (in red – contacts with the terminal arginine residue, in blue – contacts with the penultimate hydrophobic residue), also shown in (C). Residues are numbered according to the UBR5 sequence.

C Electrostatic potential surface representation of the UBR5 and UBR2 (PDB:3NY3) UBR boxes. UBR5 residues corresponding to the residues mediating the N-degron binding in UBR2 are highlighted.

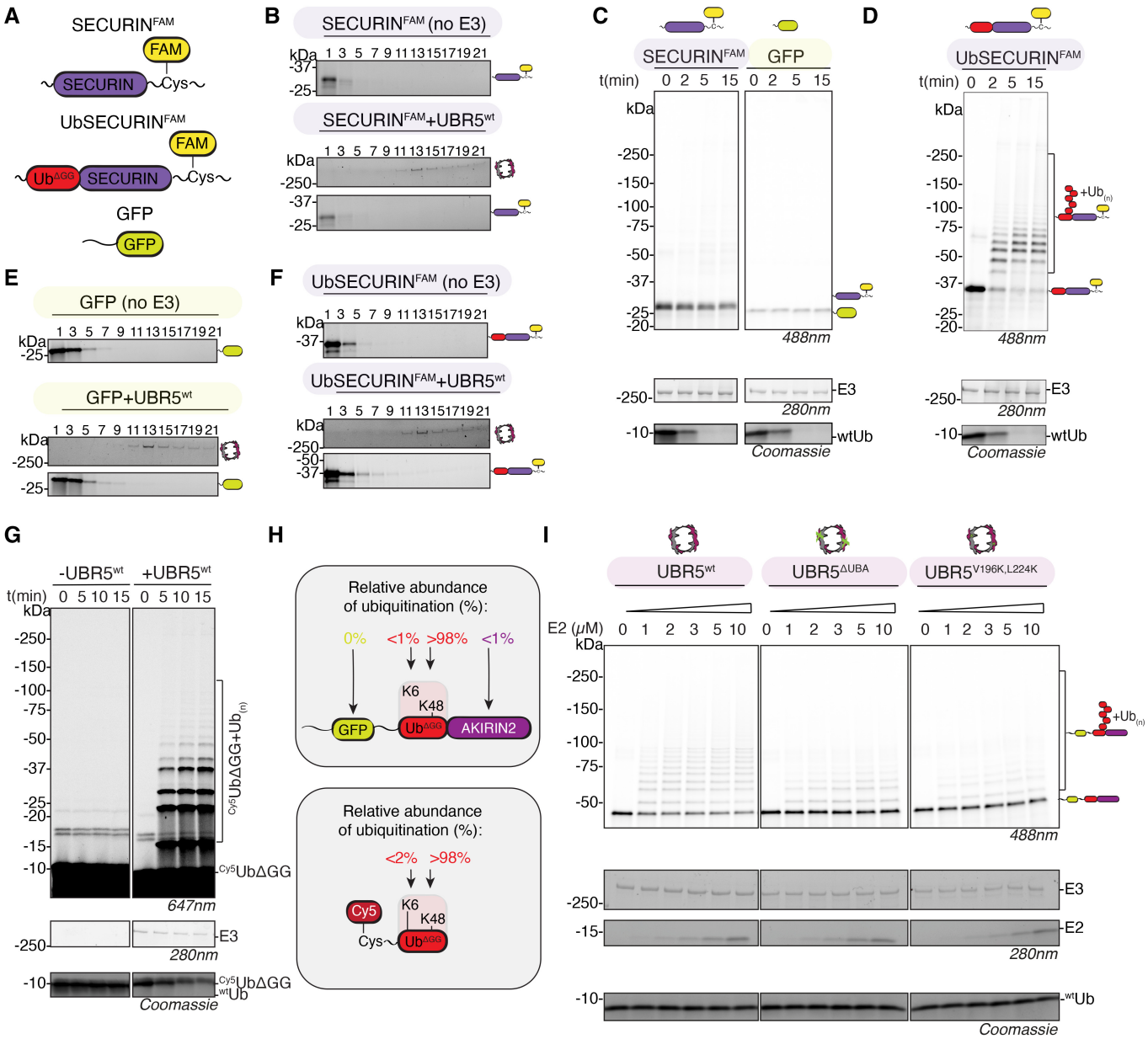

Figure EV3. Substrate selection of UBR5.

A A schematic representation of control substrates used in activity assays and complex reconstitutions.
B Sucrose gradient sedimentation profiles of control substrate SECURIN^{FAM} in the presence or absence of UBR5.
C Ubiquitination of control substrates GFP and SECURIN^{FAM}.
D Ubiquitination of UbSECURIN^{FAM}.
E Sucrose gradient sedimentation profiles of GFP control.
F Sucrose gradient sedimentation profiles of control substrate UbSECURIN^{FAM} in the presence or absence of UBR5.
G Ubiquitination assays of ^{Cy5}UbΔGG in the presence or absence of UBR5.
H A schematic representation of the chain types and relative chain abundance formed by UBR5 on two substrates, identified using mass spectrometry.
I Ubiquitination activity of UBR5 constructs with a gradual increase of the E2 concentration. Wild-type and two mutant UBR5 constructs, UBR5$^{\Delta UBA}$ and UBR5$^{V196K, L224K}$ (residues highlighted in Fig EV2A–i) ubiquitination activity was compared on ^{GFP}UbAKIRIN2 substrate using a range of 0–10 μM of UBCH5B.

Data information: Gels were imaged using fluorescent imaging (488 or 647 nm, for FAM and Cy5, respectively) to detect substrates and stain-free imaging to visualise all proteins. Gels were subsequently stained using Coomassie staining to visualise ubiquitin levels. Gels of assays are a representative of at least two experimental replicates. Reactions in C, D, G were performed at 37° and at 25° in I. All reactions contained a final concentration of 0.3 μM E3.
Source data are available online for this figure.

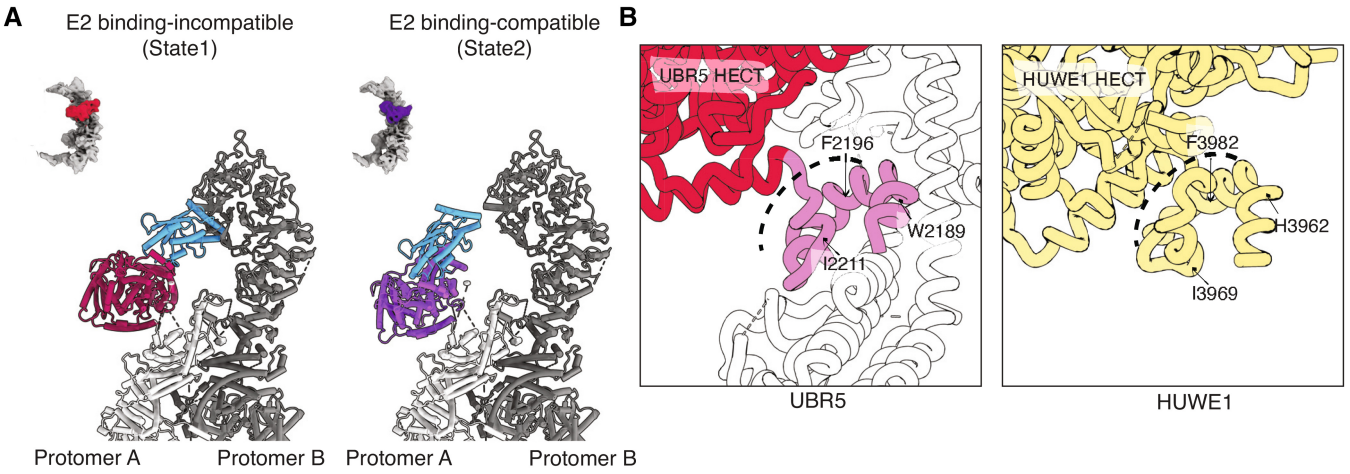

Figure EV4. Features of the HECT domain.

A Positions of UBCH5B (in blue) when docked onto UBR5 HECT domain in State 1 (left) and State 2 (right) identified by 3DVA. UBCH5B docking was guided by the NEDD4-2-UBCH5B crystal structure (PDB:3JVZ) to the conserved E2-binding motif on the HECT domain.
B A comparison of the UBR5 (in red and pink) and HUWE1 (in gold, PDB:7MWD) hinges from full-length structures. Dashed lines represent the border between the hinge and HECT domains.